BNL-TR-597

THEORY OF MAGIC NUCLEI

V.G. Nosov and A.M. Kamchatnov

The Kurchatov Institute of Atomic Energy
IAE-2286

Moscow, 1973

ABSTRACT

A consistent theory of the shell and magic oscillations of the masses of spherical nuclei is developed on the basis of the Fermi liquid concept of the energy spectrum of nuclear matter. A "magic" relationship between the system's dimensions and the limiting momentum of the quasi-particle distribution is derived; an integer number of the de Broglie half-waves falls on the nuclear diameter. An expression for the discontinuity in the nucleon binding energy in the vicinity of a magic nucleus is obtained. The role of the residual interaction is analyzed. It is shown that the width of the Fermi-surface diffuseness due to the residual interaction is proportional to the squared vector of the quasi-particle orbital angular momentum. The values of the corresponding proportionality factors (the coupling constant for quasi particles) are determined from the experimental data for 52 magic nuclei. The rapid drop of the residual interaction with increasing nuclear size is demonstrated.

1. INTRODUCTION

The nucleus was initially studied as a macroscopic body by Weizsäcker.[1] His semiempirical equation, refined by Bethe[2] and Fermi,[3] allowed a fairly accurate description of the total binding energies of many nuclei. This, however, led to many digressions from his original equation, a problem that has arisen repeatedly in one form or another during the past 35 years. The most plausible explanation for the departure from Weizsäcker's equation is that the protons and neutrons can be added to a nucleus only in whole numbers. The general belief, however, that the so-called magic and shell discrepancies are not macroscopic in origin[4,5] is more a dogmatic assertion than a fact directly following from experiment. Theoretical study of the macroscopic properties of a substance, which is closely connected with experimental observation of the thermodynamic properties, allows effects such as the phase transition to be observed and carefully analyzed. The specific property of a nucleus is its direct accessibility to absolute zero temperature (the ground state), and its energy, i.e., nuclear mass, is the most important thermodynamic value. Judging from the experimental data shown schematically in Fig. 1, the characteristic features of interest apparently are "kinks," i.e., discontinuities in the derivative of the energy of the particles. The sluggish, almost horizontal part of the curve represents the region of nonspherical nuclei and the Curie point corresponds to the phase transition analyzed by Nosov,[17] which

changes in particular the equilibrium shape of the nucleus. Figure 1 also shows the magic "cusps" of spherical nuclei, downward pointing spikes whose peaks contain appropriate magic nuclei. Note the difference between this characteristic feature and the ordinary Curie point. A qualitative difference between the phases - different values of the chemical potential - can occur only near such an "isolated" transition point. At some distance from this point, however, one phase could not have a characteristic that the other lacked. Since the solid itself shows no evidence of a discontinuity (on the macroscopic scale; see next section), it could be said that in some respects we have a second-order transition.

The traditional explanation of magic numbers[4,5] uses the concept of fermion occupation of the $2j + 1$ degenerate, single-particle levels in a spherically symmetric potential well. After a shell has been filled, the next nucleon approaches the lower edge of the continuous spectrum, and the nucleon binding energy ε (the chemical potential of opposite sign) decreases accordingly. The weakness of this interpretation is that an analogous situation should occur after each individual level, rather than a specific group of levels, has been filled. In contrast to the spacing between the neighboring shells, the level spacing within each shell cannot always be small, since such a small, dimensionless parameter cannot be obtained. Specific calculations of single-nucleon level schemes confirm the validity of this assumption (see, for example, the neutron energy-level diagram in Ref. 8). We should observe a whole series of cusps corresponding to each level.

In fact, in Fig. 1 medium weight nuclei beyond the magic number 28 exhibit cusps that correspond to much less frequently occurring true magic numbers.

Furthermore, only some of the characteristics of the well of interest can be clearly determined: the location of the well's bottom is not a strict quantitative concept because of the strong attenuation of the deep-lying quasi particles. This theoretical assumption has been confirmed by experimental data on the knockout of the deep-lying protons from nuclei.[9] The difference between the real Fermi liquid and the simple Fermi-gas model in an external field is schematically shown in Fig. 2. In both cases we deal with the quasi-particle energy if it is measured from zero kinetic energy of the free outer nucleon. At the Fermi distribution limit this value reduces to the chemical potential $\epsilon_f = -\epsilon$, where ϵ is the nucleon binding energy. Furthermore, in the example shown in Fig. 2a the energy ϵ', which is measured from the potential well's bottom, determines the limiting momentum $p_f = k_f R \sim \sqrt{\epsilon'_f}$ (R is the radius of the well). However, noninteracting quasi particles can exist in the nuclear Fermi liquid (see Fig. 2b) only in the immediate vicinity of the Fermi level, and ϵ'_f drops out. The concept of limiting momentum nonetheless remains important. Theoretically we could estimate the value of p_f from the wave function of the last quasi particle. The theory developed in the next sections is based on the crucial assumption that the limiting momentum p_f is de·ermined by the total number

of particles N:

$$N = N(\rho_f) \tag{1}$$

(the specific function can be found in Sections 2 and 5).

The total energy of the nucleus vs. ρ_f (or N) undergoes oscillations because of the density oscillations of the single quasi-particle states near ρ_f. The latter are ultimately dependent on the conservation of the orbital angular momentum ℓ in spherical nuclei, and the eigenvalues $\rho = kR$ can be graphically represented by points on the plane ℓ, ρ. Figure 3 clearly shows their grouping in the region of intermediate orbital angular momenta for

$$\rho \gg 1. \tag{2}$$

Here the Regge trajectories constructed according to the $2n + \ell = p$ rule (n is the principal quantum number and p is the number of the trajectory) are situated near the peak, where their shape is determined by

$$\Delta \rho = - \frac{(\ell + \frac{1}{2})^2}{2\rho} \tag{3}$$

(see Appendix).

The spacing between the curves, equal to $\pi/2$ along the Y axis, is the spacing between the neighboring shells in the ρ scale.[*] Let us assume that the Fermi level

$$\rho = \rho_f \qquad (4)$$

advances, say, upward. After exhausting the levels of the last Regge trajectory at the point of tangency (see Fig. 3), the density of states $d\tilde{N}/d\rho$ ($\tilde{N}$ is the number of single quasi-particle states situated below the ρ level) decreases rapidly. In a more formal sense, this can be attributed to the oscillating part $\tilde{N}_1(\rho)$ of the $\tilde{N}(\rho)$ function (see Ref. 11), whose period is determined by the spacing between the trajectories in Fig. 3. Thus, the oscillating part E_1 of the total energy $E = E_0 + E_1$ of the nucleus (E_0 is the part of the energy depending on ρ_f) is given by

$$E_1(\rho_f) = -\varepsilon \tilde{N}_1(\rho_f), \qquad (5)$$

---

[*] In connection with Fig. 3 it is interesting to point out a simple experimentally confirmed corollary: each nuclear shell contains either one s- or one p-state, and the single-particle levels of similar energy are situated near the end of the closure of this shell. Spatially inhomogeneous atomic structure in this respect is more complex and has no similar theorem; see, for example, Ref. 12.

where the factor of proportionality ϵ is the first variational energy derivative of the distribution function[13,14] or, in other words, the energy of a quasi particle near the Fermi level.

The oscillating part $\tilde{N}_1(\rho_f)$ can be determined by calculating the number of single quasi-particle states occupied by fermions, according to the Poisson equation[15]

$$\sum_{n=0}^{\infty} \varphi(n) = \frac{1}{2}\varphi(0) + \int_{0}^{\infty} \varphi(n)dn + \sum_{\nu=1}^{\infty} \int_{0}^{\infty} (e^{i2\pi\nu n} + e^{-i2\pi\nu n})\varphi(n)dn. \quad (6)$$

The dominant contribution to the last oscillating term comes from quasi particles nearest to the Fermi distribution level (graphically represented in Fig. 3). In fact, the oscillating integral under the summation over ν would be too small for a smooth $\varphi(n)$ function. However, in calculating the thermodynamic functions of the Fermi systems, $\varphi(n)$ should contain in the form of a multiplier the statistical distribution of quasi particles, which changes sharply in the neighborhood of the Fermi level. An example of such an oscillating characteristic in "ordinary" Fermi systems is the de Haas-van Alphen effect in metals.[16,17] The finite size of the nucleus apparently cannot be canonically transformed to such quasi particles, for which expression (4) for an ideally sharp, stepwise Fermi distribution would hold. This is commonly known in nuclear physics as the "residual" interaction between nucleons. The diffuse Fermi level resulting from it will generally suppress the oscillations. However, only a

certain type of diffuse Fermi level qualitatively corresponds to experimental data. For example, the statistical temperature distribution

$$w_T = \frac{1}{e^{\frac{P-P_f}{\tau}} + 1} \qquad (7)$$

yields an analytic expression for $\widetilde{N}_\ell(\rho_f)$ without magic cusps.[*]

What quantities or functions characterize the residual interaction? We can imagine, of course, a case in which the residual interaction between quasi particles is described by a specific Hamiltonian: one such model is calculated in Section 3. However, we should consider that, although because of the interaction the energy of the individual quasi particle, strictly speaking, is no longer a precisely defined quantity, Eq. (5) can still be used for the approximation of interest. Suppose the region of the diffuse Fermi distribution determined by the residual interaction has the width $\delta\epsilon$ - this of course can be considered the uncertainty in the quasi particle's energy of the same order of magnitude. On the other hand, in the ρ scale (see Fig. 3 and next section), $\delta\rho$ characteristic of oscillations is of the order of unity. Therefore, in the region of oscillations, $\delta\epsilon \approx (d\epsilon/d\rho)\delta\rho \approx \epsilon/\rho_f$. Taking into

---

[*] This remark can be considered as the corollary of a more general theorem. It is clear that continuous distributions of quasi particles with respect to the states, which are independent of ℓ, exhibit no cusplike characteristics. The dependence of the width of the diffuse Fermi distribution on the quantum number ℓ, compatible with the experimentally observed magic cusps, is determined in Sections 3 and 4.

account Eq. (2), we get

$$\delta\varepsilon \ll \varepsilon, \qquad\qquad (8)$$

i.e., the first factor on the right-hand side of Eq. (5) can be determined with sufficient accuracy. In other words, the redistribution of quasi-particle states as a result of the residual interaction should be determined in principle from the minimum energy of the nucleus. The oscillations can then be calculated, neglecting the additional energy of interaction between quasi particles. The specific example in Section 3 illustrates this curious feature.

The so-called dynamic approach - here we mean the specific Hamiltonian for interaction between quasi particles - is highly ambiguous. Since a canonical transformation giving a sharp Fermi level [Eq. (4)] does not exist, we cannot choose unambiguously a transformation for a new, quasi-particle Hamiltonian. According to Eq. (8), the residual interaction can be more adequately described by the distribution function for quasi particles. If we consider this function $w(p,\mathcal{E})$ a primary concept in a certain sense of the word, it would seem possible to use its simple single-parameter approximations. In this case, it would be possible to observe such a characteristic feature as a rapid decrease of the residual interaction with increasing nuclear size. The problems considered here will be discussed in the final sections of this

paper, and the theory in which the residual interaction is neglected, i.e., one with a sharp Fermi level [Eq. (4)], will be discussed in the next section.

2. SHELL STRUCTURE OF A SPHERICAL NUCLEUS IN THE ABSENCE OF RESIDUAL INTERACTION

An asymptotic expression of the function $N = N(\rho_f)$ for large ρ_f's [see Eqs. (1) and (2)] must be terminated after a finite number of terms:

$$N(\rho_f) = \frac{2 \cdot 2}{9\pi} \rho_f^3 - s\rho_f^2 + q\rho_f. \tag{9}$$

In fact, the fifth term of the expansion $\sim \rho_f^{-1}$ would add physically meaningless fractional parts to the particles. A macroscopic approach apparently requires that the fourth term describing the "single-particle effect" be also dropped (see Introduction). All nonmacroscopic terms such as $\rho_f^0 \approx 1$ will henceforth be dropped. The third term in Eq. (9) may also seem incorrect, since $2\ell + 1 \approx \rho_f$ particles would populate a single level in a spherically symmetric field (see Introduction). However, the zero-point oscillations of the deformation α have a scale $\Delta\alpha \approx \rho_f^{-2}$, which is also the order of magnitude of the relative shift of the quasi-particle energy (this effect was pointed out by Rainwater[18]). As a result, the degeneration of energy diminishes to a sufficient degree, but such small

deformations do not violate the conservation of the integral of
motion l (see Ref. 19). Thus, the $N(\rho_f)$ function implicit in
Eq. (9) averages out automatically in the actual situation. Taking
into account additional spin doubling, the coefficient of the first
term on the right-hand side of Eq. (9) corresponds to the volume
contribution to the cells in the phase space; i.e., it is equal to
the specific expression for the ideal Fermi gas.[*]

The surface term $s\rho_f^2$ and the "curvature term" $q\rho_f$ take into
account the structure of the transition layer at the nuclear surface,
the spin-orbit coupling within the nucleus, etc. The numerical
values of the coefficients s and q must be determined experimentally
(see Section 5).

We shall initially calculate the oscillating part $\widetilde{N}_1(\rho_f)$ of the
single quasi-particle levels in a rather straightforward manner by
using the model[19] for the gas situated in a well with a constant
potential (this physically corresponds to a homogeneous spatial
distribution of matter within the nucleus). To calculate $\widetilde{N}_1(\rho_f)$,
one must sum over l and n the quantity[†]

$$\varphi(\ell, n) = 2\,(2\,\ell + 1)\, w_f(\ell, n). \tag{10}$$

---

[*] Only in this volume approximation can $\widetilde{N}(\rho_f)$ be identified with
the number N of true particles. This approximation, however, is
too crude for nuclear physics.

[†] Because of the macroscopic character of the effect being studied,
the spin of the nucleon is determined by simple doubling. Note
that at this step of the calculation the principal quantum number
n should be numbered from zero rather than unity. For example,
n = 0 is assigned to the 1s state. This will make it possible to
use Eq. (6) in summing over both quantum numbers [see Eq. (14)
below].

Owing to the eigenvalues $\rho = \rho_{\ell n}$ the Fermi distribution

$$w_f(\ell, n) = \begin{cases} 1 & \text{when } \rho_{\ell n} < \rho_f, \\ 0 & \text{when } \rho_{\ell n} > \rho_f \end{cases} \qquad (11)$$

depends on the same quantum numbers. The eigenvalues can be deter-mined by using the Bohr-Sommerfeld quantization rule [12]:

$$\int_a^R k_\ell(r)\, dr = \pi\,(n + \gamma), \qquad (12)$$

where the internal turning point r = a is determined by the centri-fugal barrier and γ < 1 determines the additional phase that depends on the boundary conditions. Integral (12) need not be recalculated because the wave functions (spherical Bessel functions) and their quasi-classical asymptotic behavior are well known. Confining our-selves to notations used in Ref. 19, we get

$$\rho\,(\sin\beta - \beta\cos\beta) = \pi\,(n + \tfrac{3}{4}),$$

$$\beta = \arccos\frac{\ell + \tfrac{1}{2}}{\rho}, \qquad dn\,d\ell = \frac{\rho\,d\rho}{\pi}\sin^2\beta\,d\beta. \qquad (13)$$

A double summation of function (10) according to Eq. (6) yields

$$\sum_{n=0}^{\infty}\sum_{\ell=0}^{\infty}\varphi(\ell,n) = \frac{1}{4}\varphi(0,0) + \sum_{\nu=1}^{\infty}\iint_0^\infty (e^{i2\pi\nu n} + e^{-i2\pi\nu n})\varphi(\ell,n)d\ell dn +$$

$$+ \sum_{\lambda=1}^{\infty}\iint_0^\infty (e^{i2\pi\lambda\ell} + e^{-i2\pi\lambda\ell})\varphi(\ell,n)d\ell dn +$$

$$\frac{1}{2}\left\{\int_0^\infty \varphi(0,n)dn + \sum_{\nu=1}^{\infty}\int_0^\infty (e^{i2\pi\nu n} + e^{-i2\pi\nu n})\varphi(0,n)dn\right\} + \qquad (14)$$

$$\frac{1}{2}\left\{\int_0^\infty \varphi(\ell,0)d\ell + \sum_{\lambda=1}^{\infty}\int_0^\infty (e^{i2\pi\lambda\ell} + e^{-i2\pi\lambda\ell})\varphi(\ell,0)d\ell\right\} + \iint_0^\infty \varphi(\ell,n)d\ell dn +$$

$$\sum_{\lambda=1}^{\infty}\sum_{\nu=1}^{\infty}\iint_0^\infty [e^{i2\pi(\lambda\ell+\nu n)} + e^{-i2\pi(\lambda\ell+\nu n)} + e^{i2\pi(\lambda\ell-\nu n)} + e^{-i2\pi(\lambda\ell-\nu n)}]\varphi(\ell,n)d\ell dn.$$

Equation (14) contains two radically different types of integral. Although those that depend on almost the entire range of values $0 < \rho = kR < \rho_f$ of a particle's wave number cannot be generalized to the real Fermi liquid, they depend smoothly on ρ_f and can be dropped. The integrals oscillating as a function of ρ_f rapidly converge at $\rho \approx \rho_f$ and can be generalized to the Fermi liquid. The importance of the lower part of the scale of angular momenta, where $\beta \approx \pi/2$, is evident from Fig. 3 (see Introduction). There-

fore, the additional angle should be introduced for conveni⋅ ⋅ce:

$$\tilde{\beta} = \frac{\pi}{2} - \beta. \tag{15}$$

All the terms on the right-hand side of Eq. (14) can now be easily classified according to the criteria defined above. The nonmacroscopic character of the first term is evident; after integration, one can see that the second term also lacks macroscopic characteristics. After integration according to Eqs. (13) and (15) and summation over λ, we can see that the third term, equal to $p_f/6\pi$, depends smoothly on the limiting momentum. This also applies to the two following pairs of terms enclosed in braces.

The oscillations are described by the double summation over λ and ν ⌜the last term in Eq. (14)⌝. The integral under the summation sign has essentially the same structure as the second term on the right-hand side of Eq. (14); i.e., it is nonmacroscopic. However, for a specific relationship between λ and ν, a saddle point yielding a macroscopic contribution will occur at the lower edge of the momentum axis (i.e., at $\tilde{\beta} = 0$; see also Fig. 3).

Taking Eqs. (13) and (15) into account, we can write the expansion of the argument of the exponential in powers of $\tilde{\beta}$ up to the quadratic terms:

$$2\pi(\lambda\ell + \nu n) \cong -\pi\lambda - \frac{3}{2}\pi\nu + 2\nu\rho + \pi(2\lambda - \nu)\rho\tilde{\beta} + \nu\rho\tilde{\beta}^2. \tag{16}$$

The linear term (the condition for the existence of the saddle at $\widetilde{\beta} = 0$) vanishes at

$$\nu = 2\lambda. \tag{17}$$

Thus, using (10), (11), (13), and (15), we get

$$\int\int_0^\infty e^{i2\pi(\lambda\ell + \nu n)} \varphi(\ell, n)\, d\ell\, dn \cong \frac{4}{\pi} \int_0^{\rho_f} d\rho\, \rho^2 e^{i4\lambda\rho} \int_0^{\frac{\pi}{2}} e^{i2\lambda\rho_f\widetilde{\beta}^2}\, \widetilde{\beta}\, d\widetilde{\beta} \cong \frac{\rho_f}{4\pi}\, \frac{e^{i4\lambda\rho_f}}{\lambda^2}. \tag{18}$$

Addition of a complex conjugate expression and summation over the only remaining free index yields

$$\widetilde{N}_1 = \frac{\rho_f}{2\pi} \sum_{\nu=1}^{\infty} \frac{\cos 4\nu\rho_f}{\nu^2}. \tag{19}$$

For the oscillating part of the energy of the nucleus E_1, we use Eq. (5):

$$E_1 = -\varepsilon \frac{\rho_f}{2\pi} \mathcal{M}(\rho_f). \tag{20}$$

Thus, when the quasi particles have a sharp, steplike Fermi level (this occurs in the absence of residual interaction between them; see Introduction), the shell effects are described by a universal periodic function,

$$\mathcal{M}(\rho_f) = \sum_{v=1}^{\infty} \frac{\cos 4 v \rho_f}{v^2},\qquad (21)$$

whose plot is shown in Fig. 4. The derivative of this function is discontinuous when the values of its argument are

$$k_f R = \frac{\pi}{2} p,\qquad p = 2,3,4,5...,\qquad (22)$$

which correspond to the magic cusps. Since $\rho_f = \pi$ corresponds to the 1s state (the doubly magic nucleus $_2\text{He}_2^4$ can be used as an example), the magic numbers p should begin with number 2.*

---

* The definition of the effective nuclear radius R implied in Eq. (22) pertains to its internal structure. Since we are using a model with an impenetrable wall,[19] we must imagine it to be at the point where the wave function of a given quasi particle extrapolated from the inner region vanishes. In other words, the effective nuclear surface can always be treated in such a way that the additional phase arising from the Bohr-Sommerfeld rule[12] will have the value $\gamma = 3/4$ for the dominant quasi particles, in accordance with Eq. (13) (see Introduction). In close connection with this fact, the equations expressing the shell oscillations in terms of ρ_f are universal and do not depend on the spin-orbit interaction or the structure of the surface layer. On going to the N-scale, however, this universality is lost [see Eq. (9) and its explanation].

We can see that the right-hand side of Eq. (21) is a Fourier series for the elementary function which we explicitly write in a form valid for the two periods adjoining the magic nucleus p:

$$\mathcal{M}(\rho_f) = \frac{\pi^2}{6} - 2\pi \left| \rho_f - \frac{\pi}{2}p \right| + 4\left(\rho_f - \frac{\pi}{2}p\right)^2, \quad (23)$$
$$\frac{\pi}{2}(p-1) < \rho_f < \frac{\pi}{2}(p+1).$$

The absolute-value symbol indicates the nonanalyticity of the function at the magic cusp. Using the symbols + and - to distinguish the values of the discontinuous function on the right-hand and left-hand sides respectively, we have

$$\left(\frac{d\mathcal{M}}{d\rho_f}\right)_{\pm} = \mp 2\pi. \quad (24)$$

And now, returning to (20), we obtain an expression for the discontinuity in the derivative of the oscillating part of the energy of the nucleus:

$$\Delta\left(\frac{dE_f}{d\rho_f}\right) = \rho_f(\mathcal{E}_+ + \mathcal{E}_-) = 2\rho_f \overline{\mathcal{E}}. \quad (25)$$

To proceed from the limiting momentum to the true number of particles [Eq. (1)], both sides of the equation must be multiplied by $d\rho_f/dN$.

Note that the smooth component E_o has no singularities at the cusp, so that Eq. (25) actually gives the discontinuity in the derivative of the total energy E:

$$\Delta\left(\frac{dE}{dN}\right) = \bar{\varepsilon}\ \frac{d\rho_t^2}{dN}. \qquad (26)$$

This relation can also be considered the equation for the discontinuity of the nucleon binding energy $\varepsilon = -dE/dN$,

$$\Delta\varepsilon = \bar{\varepsilon}\ \frac{d\rho_t^2}{dN} \qquad (27)$$

in the vicinity of the magic nucleus. Thus, we can assume that $\Delta\varepsilon = \Delta(dE/dN) = \varepsilon_- - \varepsilon_+$.

3. SIMPLE MODEL OF THE RESIDUAL INTERACTION

In choosing a model Hamiltonian we should remember that the spin of an even-even nucleus in the ground state is equal to zero and, within the limits of the shell-model representation, the spin of the odd nuclei always has a single particle value (see, for example, Ref. 12). We therefore have

$$H_{int}^j = -G_j \sum_{m,m'>0} a_{m'}^\dagger a_{-m'}^\dagger a_{-m} a_m \qquad (28)$$

for the interaction between quasi particles in the same j-level. Here, a_m^+ and a_m are the quasi-particle creation and annihilation operators with a z-momentum component equal to m. The Hamiltonian (28) is diagonalized exactly (see, e.g., Ref. 20); the eigenvalues are given by the well-known Racah-Mottelson equation,

$$E_{int}^j = -G_j \, b_j \, (\Omega_j - b_j + 1),$$ (29)

where $2\Omega = 2j + 1$ is the total number of vacancies, b_j is the number of interacting quasi-particle pairs with $j_z = \pm m$ at the jth level. For the nucleus, we minimize the sum

$$E = \sum_j \left[2\varepsilon_j b_j - G_j b_j (\Omega_j - b_j + 1) \right]$$ (30)

over j-levels (ε_j is the initial energy of the quasi particle) at zero point variation of the quantity

$$\tilde{N} = \sum_j 2 b_j .$$ (31)

This additional condition can be easily determined by the intermediate Lagrange multipliers. Taking into account the Pauli exclusion

principle (i.e., the condition $0 \leq b_j \leq \Omega_j$), we determine

$$w_j = \frac{b_j}{\Omega_j} = \begin{cases} 1 & \varepsilon_j - \varepsilon_f < -\frac{G_i}{2}(\Omega_j - 1), \\ \dfrac{G_i(\Omega_j + 1) - 2(\varepsilon_j - \varepsilon_f)}{2\,G_j\Omega_j} & \text{for} \quad -\frac{G_i}{2}(\Omega_j - 1) < \varepsilon_j - \varepsilon_f < \frac{G_j}{2}(\Omega_j + 1), \\ 0 & \varepsilon_j - \varepsilon_f > \frac{G_i}{2}(\Omega_j + 1), \end{cases} \tag{32}$$

where ε_f is the chemical potential. We should also take into account
the interaction energy (29) corresponding to the equilibrium division

$$E_{int}^j = \begin{cases} -G_j\Omega_j & \varepsilon_j - \varepsilon_f < -\frac{G_i}{2}(\Omega_j - 1), \\ -\dfrac{G_j^2(\Omega_j + 1)^2 - 4(\varepsilon_j - \varepsilon_f)^2}{4G_j} & \text{for} \quad -\frac{G_i}{2}(\Omega_j - 1) < \varepsilon_j - \varepsilon_f < \frac{G_i}{2}(\Omega_a + 1), \\ 0 & \varepsilon_j - \varepsilon_f > \frac{G_i}{2}(\Omega_j + 1). \end{cases} \tag{33}$$

In a macroscopic analysis used here, $\Omega_j \pm 1$ is replaced by $\Omega_j = j + 1/2$,
the quasi particle's orbital angular momentum ℓ is substituted for its
momentum j to within the same accuracy, and the spin-orbit interaction
is omitted. Let us consider more appropriate variables (13) and (15):

$$\Omega_j \cong \rho \sin\tilde{\beta} \cong \rho_f\,\tilde{\beta}, \quad \tilde{\beta} = \text{arc}\sin\frac{\tilde{\ell}}{\rho}, \quad \tilde{\ell} = \ell + \frac{1}{2}, \tag{34}$$

$$G_j = \frac{d\varepsilon}{d\rho}\Big|_f \cdot g_j.$$

It is assumed here that the small $\tilde{\beta}$'s are essential for oscillations.
In this limit the $\tilde{\beta}$ dependence of the coupling constant is exponential:

$$g_j = g\beta^{k-1} \tag{35}$$

In the variables ρ and $\tilde{\beta}$ distribution (32) has the form

$$w(\rho,\tilde{\beta}) = \begin{cases} 1 & \rho-\rho_f < -\frac{g}{2}\rho_f\tilde{\beta}^\kappa, \\ \frac{1}{2} - \dfrac{\rho-\rho_f}{g\rho_f\tilde{\beta}^\kappa} & \text{for} \quad -\frac{g}{2}\rho_f\tilde{\beta}^\kappa < \rho-\rho_f < \frac{g}{2}\rho_f\tilde{\beta}^\kappa, \\ 0 & \rho-\rho_f > \frac{g}{2}\rho_f\tilde{\beta}^\kappa \end{cases} \quad (36)$$

(see Fig. 5). On the basis of the results of the preceding section, we conclude that

$$\tilde{N}_f = \sum_{\nu=f}^{\infty} (\tilde{N}^\nu + \tilde{N}^{\nu*}),$$

$$\tilde{N}^\nu = \iint_0^\infty e^{i\nu 2\pi(2n+\ell)} \cdot 2(2\ell+1)\, w(\ell,n)\, d\ell\, dn \cong \qquad (37)$$

$$\frac{4}{\pi}\rho_f^2\, e^{i\nu 4\rho_f} \int_0^\infty d\tilde{\beta}\cdot\tilde{\beta}\, e^{i\nu 2\rho_f\tilde{\beta}^2} \int_{-\infty}^\infty w(\rho,\tilde{\beta})\, e^{i\nu 4\xi}\, d\xi \qquad \xi=\rho-\rho_f$$

in the general case. After simple integration over ξ, we get

$$\tilde{N}^\nu = -\frac{\rho_f\, e^{i\nu 4\rho_f}}{4\pi g\nu^2} \int_0^\infty e^{i\nu 2\rho_f\tilde{\beta}^2}\left(e^{i\nu 2g\rho_f\tilde{\beta}^\kappa} - e^{-i\nu 2g\rho_f\tilde{\beta}^\kappa}\right) \frac{d\tilde{\beta}}{\tilde{\beta}^{\kappa-1}}. \quad (38)$$

To determine the values of the power of k compatible with experimental data, we should consider the extreme case in which the convergence of the integral (38) is determined mainly by the term proportional to g in the exponential. After expanding the other exponential function $e^{i\nu 2\rho_f\tilde{\beta}^2}$ in a series, we confine ourselves to the first two terms and substitute them in Eq. (37); taking Eq. (5) into account, we obtain an

expression for the oscillating part of the energy (the energy of each quasi particle is assumed to be equal to $-\epsilon$; see conclusion of this section):

$$E_1 \cong -\frac{\epsilon \rho_f}{\pi \kappa g}\left\{ \frac{(2g\rho_f)^{2-\frac{4}{\kappa}}}{g} \int_0^\infty \frac{\sin y\,dy}{y^{2-\frac{4}{\kappa}}} \sum_{\nu=1}^\infty \frac{\cos 4\nu\rho_f}{\nu^{\frac{4}{\kappa}}} + \right.$$

$$\left. + (2g\rho_f)^{1-\frac{2}{\kappa}} \int_0^\infty \frac{\sin y\,dy}{y^{2-\frac{2}{\kappa}}} \sum_{\nu=1}^\infty \frac{\sin 4\nu\rho_f}{\nu^{1+\frac{2}{\kappa}}} \right\}, \qquad g \gg \rho_f^{\frac{\kappa}{2}-1}. \tag{39}$$

Expression (39) is distinguishable by its trigonometric series, which can be easily analyzed. A cusplike singularity (i.e., finite discontinuity of the derivative $dE/d\rho_f$; see Fig. 1) is capable of yielding only an even cosine series with respect to $t = 4\rho_f - 2\pi p$. At $k < 2$ we have $4/k > 2$, and the derivatives converge uniformly according to the Weierstrass convergence test. Thus, at $k < 2$ there are no cusps,[*] and at $k > 2$ they are pronounced. To verify this, we shall analyze the derivative of the series of interest, which has the form $\sum_{\nu=1}^\infty \sin\nu t/\nu^\alpha$, where $\alpha < 1$. Near the singular point we have $\sin\nu t \approx \nu t$ up to the limit $\nu = \tilde{\nu} \approx 1/|t|$. Substituting integration for summation, we determine

$$\sum_{\nu=1}^\infty \frac{\sin\nu t}{\nu^\alpha} \sim t \int_0^{\tilde{\nu}} \nu^{1-\alpha}d\nu \sim t\,\tilde{\nu}^{2-\alpha} \sim \frac{t}{|t|^{2-\alpha}}. \tag{40}$$

---

[*] In the special case of $k = 0$, the absence of cusps is clearly evident.

Consequently, at k > 2 and $\alpha = \frac{4}{k} - 1 < 1$, the derivative of the first term in Eq. (39) has an infinite discontinuity at t = 0 [Eq. (40) is consistent with the rigorous mathematical theorems; see, for example, Ref. 21]. Thus, only

$$K = 2 \tag{41}$$

is compatible with the experimentally observed magic cusps. To eliminate g >> 1 bounded from below for the coupling constant, we should substitute (41) in (38) and integrate. Finally, we obtain

$$E_1 = -\frac{\varepsilon \beta_1}{2\pi} \left\{ f_1(g) \, \mathcal{M}(\beta_1) + f_2(g) \, \mathcal{N}(\beta_1) \right\}, \tag{42}$$

where

$$f_1(g) = \frac{1}{2g} \ln \left| \frac{1+g}{1-g} \right|,$$

$$f_2(g) = \frac{\pi}{2g} \theta(g-1),$$

$$\theta(x) = \begin{cases} 1 & \text{when } x > 0, \tag{43a} \\ 0 & \text{when } x < 0 \tag{43b} \end{cases}$$

are the functions whose plots are shown in Fig. 6. Here we also have the function

$$\mathcal{M}(\rho_f) = \sum_{\nu=1}^{\infty} \frac{\sin 4\nu\rho_f}{\nu^2}, \tag{44}$$

characteristic of oscillations in the presence of a residual inter-action. This function approaches zero at the cusp. Differentiating (42), we obtain the discontinuity

$$\Delta\mathcal{E} = \overline{\mathcal{E}} \frac{d\rho_f^2}{dN} f_1(g) \tag{45}$$

for the nucleon binding energy in the nucleus. According to (43), this discontinuity approaches infinity as $g \to 1$. Physically, this is attributed to the fact that at $g = 1$ one of the boundaries of the interaction region II [see Eq. (36) and Fig. 5] is superimposed on the Regge trajectories [see Eq. (3) and Fig. 3]. However, such a sharply defined region of intermediate occupation numbers is not likely to exist. In fact, the coefficient of the $m(\rho_f)$ function presumably should nowhere become infinite. Note that a simple inter-polation equation can be obtained for the $f_1(g)$ function. Since $f_1 \to 1$ as $g \to 0$ in the absence of residual interaction [Eq. (27)], and in the asymptotic region ($g \gg 1$) according to (43) $f_1 \simeq 1/g^2$, we get

$$f_1(g) \approx \frac{1}{1+g^2} \cdot \qquad (46)$$

The discontinuity $(\Delta \epsilon)_0$ in the absence of residual interaction [see Eq. (27)] differs from that in Eq. (45) by

$$\omega \equiv \frac{(\Delta \epsilon)_0}{\Delta \epsilon} - 1 = \frac{1}{f_1(g)} - 1 \approx g^2 \qquad (47)$$

(see also Ref. 11). For a crude interpolation (46) this value is expressed directly in terms of the residual interaction constant. It is more practical, however, to use the analytic or nearly analytic expressions for the $w(\rho, \tilde{\beta})$ distribution function. One such example is analyzed in the next section.

We now can analyze the assumption made above that each quasi particle has a specific energy ϵ, distinct from the energy [Eq. (33)] of interaction between quasi particles, from which we get $E_1^{int} \approx \epsilon \rho_f^0 \approx \epsilon$ after a simple calculation of its oscillating part. Thus, the contribution of the interaction energy to the oscillations is not macroscopic and hence can be ignored. Since this is not an isolated case, it should in no way be considered a characteristic feature of this model. This problem has already been analyzed in

the Introduction from a general and physically more lucid point of view.

4. ANALYTIC DISTRIBUTION FUNCTION

Since the contribution of the interaction energy to the oscillations is negligible (for a given quasi-particle distribution function), the problem can be reformulated as outlined in the Introduction: the oscillating energy of the ground-state spherical nucleus is determined by the $w(\rho,\tilde{\beta})$ function (for the quasi particles of interest, it is the diagonal part of the density matrix). Strictly speaking, we cannot describe its form, although we can say that it obeys physically obvious general limitations. In the asymptotic regions it must rapidly approach zero and unity; therefore it is hard to imagine this function to be nonmonotonic. Moreover, the analysis in the preceding section [see Eqs. (41) and (42)] suggests that only the quadratic dependence on the orbital angular momentum of the diffuse Fermi-distribution width can be reconciled with the experimentally observed magic effects for any intensities of the residual interaction. In fact, it can be easily shown that for any distributions of the type $w(\rho-\rho_f/\tilde{\beta}^2)$ the oscillating part of the energy E_1 can always be reduced to a linear combination of $m(\rho_f)$ and $n(\rho_f)$. We should therefore use the ordinary Fermi distribution function [Eq. (7)] with the modulus quadratically dependent on the angle $\tilde{\beta}$

$$w(\rho, \tilde{\beta}) = \frac{1}{e^{\frac{\rho - \beta_f}{\tau \tilde{\beta}^2}} + 1}. \qquad (48)$$

Calculation of the oscillating part of the energy E_1 according to Eqs. (5) and (37) yields

$$E_1 = -\frac{\varepsilon \beta_f}{2\pi} \left\{ F_1(g) \, \mathcal{M}(\beta_f) + F_2(g) \, \mathcal{N}(\beta_f) \right\},$$

$$F_1(g) = \frac{1}{2\pi g} \int_0^\infty \frac{\sin \frac{u}{\pi g}}{sh \frac{u}{2}} u \, du, \qquad (49)$$

$$F_2(g) = \frac{1}{2\pi g} \int_0^\infty \frac{\cos \frac{u}{\pi g}}{sh \frac{u}{2}} u \, du = -\frac{\frac{\pi}{2g}}{ch^2 \frac{1}{g}}$$

(it is assumed here that $\tau = 1/4g\rho_f$; the advantage of this designation will become clear later). The plots of the $F_1(g)$ and $F_2(g)$ functions are shown in Fig. 7. As in examples (36) and (41), the term with the $n(\rho_f)$ function is dominant in the region $g \gg 1$ of strong residual interaction; this function has the coefficient

$$F_2(g) \cong \frac{\pi}{2g}, \qquad g \gg 1. \qquad (50)$$

We chose the normalized coupling constant g (see above) so that Eq. (50) would coincide with Eq. (43b). Continuing this analogy,

we note that in the nonanalytic model (42) and (43) the term with $n(\rho_f)$ is absent when $g \ll 1$. In our case, however, this corresponds to a small exponential value in the case of weak coupling between quasi particles:

$$F_2(g) \cong \frac{2\pi}{g} e^{-\frac{2}{g}}, \qquad g \ll 1. \qquad (51)$$

Note that, in a more formal sense, the asymptotic behavior of (51) confirms the presence of a singular point at $g = 0$. It is possible that the limiting case $g \to 0$ of the sharp Fermi level has a general character.

The $m(\rho_f)$ function is solely responsible for the magic characteristics (cusps). Let us write the equations describing these characteristics:

$$\Delta \mathcal{E} = \bar{\mathcal{E}} \frac{d\rho^2}{dN} F_1(g),$$

$$\omega \equiv \frac{(\Delta \mathcal{E})_o}{\Delta \mathcal{E}} - 1 = \frac{1}{F_1(g)} - 1. \qquad (52)$$

As can be seen in Fig. 7, the $F_1(g)$ function has a maximum in the region of intermediate values of the coupling constant. Thus, the effect of interest depends nonmonotonically on the intensity of the residual interaction.

5. COMPARISON WITH EXPERIMENT

As shall use the particle scale after determining from experimental data the numerical values of the coefficients s and q in Eq. (9) for the Fermi liquid. Let us construct curve (9),

(1) through the magic numbers 50 (p = 5) and 82 (p = 6);

(2) through the magic numbers 82 (p = 6) and 126 (p = 7); and

(3) through the magic numbers 28, 50, 82, and 126 by the least-squares method. We thus obtain three sets of parameters s and q:

$$
\begin{array}{lll}
(1) & s = 1.0 & q = 5.2 \\
(2) & s = 1.1 & q = 6.8 \\
(3) & s = 1.0 & q = 5.6
\end{array}
\tag{53}
$$

The values of s and q calculated according to Eq. (9) are compared in Table 1 with the known magic numbers. Except for the very light magic nuclei, a good fit seems to begin at N = 28. However, a macroscopic analysis of magic effects is nonetheless useful in the case of light nuclei. At N and Z < 28 the observed shell correction E_1 is described by discrete points, through which a continuous curve cannot readily be drawn (see, for example, Ref. 6). The criteria for finding the magic cusps apparently disappear when condition (2) is violated. In this respect the magic numbers 2 and 8 can be thought of as an extrapolation to light nuclei of the rule given in the footnote on p. 5 [see also Eq. (22) and Fig. 3]. Note that

the agreement of the proton and neutron magic numbers indicates that the parameters s and q are practically the same for both components of nuclear matter. This is attributed to the relative smallness of the effects that distinguish a proton from a neutron in the nucleus, such as a "Coulomb curve" (radial dependence of the electrostatic potential within the nucleus).

Since nuclear matter has two constituent parts, the oscillating term can be described by the sum of expressions (49) for the neutron and proton quasi particles [*]:

$$
E_1(N,Z) = -\varepsilon_N \frac{p_F^N}{2\hbar} \left\{ F_1(q_N) \mathfrak{M}(p_r^N) + F_2(q_N) \mathfrak{M}(p_f^N) \right\} - \varepsilon_Z \frac{p_F^Z}{2\hbar} \left\{ F_1(q_Z) \mathfrak{M}(p_r^Z) + F_2(q_Z) \mathfrak{M}(p_f^Z) \right\}
\tag{54}
$$

It would be of great theoretical interest to determine the energy E(N,Z) at the location of the doubly magic nucleus. The terms proportional to m in Eq. (54) represent the surface $E_1(N,Z)$ as a pyramid of rhombic cross section with its axis directed vertically down. The terms proportional to n, however, yield a more complex shape. [*]

Let us qualitatively compare the discontinuities $\Delta\varepsilon$ of the nucleon binding energy. The values for the residual interaction constant were

---

determined from the data of Ref. 22 for 52 magic nuclei. The second
set of parameters a and q was used for the $N(p_f)$ function [see Eq. (53)].
According to the interpolation of (46) and (47), f_ω gives the most crude
characteristic of the residual interaction. The coupling constant g'
was calculated according to Eqs. (43) and (45) and g, its counterpart
in the analytic case (48), was determined from Eqs. (49) and (52). The
average values corresponding to the magic numbers 28, 50, 82, and 126
are given in Table 2.

For the shell oscillations, the $\tilde{\beta}$ dependence of the diffuse Fermi
distribution width can be controlled only up to the angles

$$2\rho_f \bar{\tilde{\beta}}^2 \sim 1,$$

(55)

after which the integrals (18) and (37) describing them converge
rapidly. According to (48), the characteristic width in the ρ scale
is given by

$$\overline{\delta\rho} = \tau \bar{\tilde{\beta}}^2 \equiv \frac{1}{4} g \rho_f \bar{\tilde{\beta}}^2 = \frac{1}{8} g.$$

(56)

We now turn to the energy scale

$$\overline{\delta\varepsilon} = \frac{d\varepsilon}{d\rho}\bigg|_f \cdot \overline{\delta\rho} = \frac{\hbar^2}{R^2} \frac{\rho_f}{m^*} \frac{g}{8}.$$

(57)

Let us assume that

$$R = 1.2 \ 10^{-13} \cdot A^{1/3} \quad \text{см} \qquad (58)$$

and that the effective mass m* of the quasi particle is equal to that of a free nucleon. The $\overline{\delta \epsilon}$ widths in megavolts are given in the last column of Table 2.

The width $\delta \epsilon$ of the diffuse region is different for specific values of the orbital angular momentum, since it is a quadratic function of ℓ. Taking (55) into account, we confine ourselves to the medium values of ℓ characteristic of the shells of interest. The results are given in Table 3.

The characteristics of the residual interaction in the tables, irrespective of their refinement and the choice of scale, consistently show that its intensity decreases rapidly with increasing size of the nucleus.

6. DISCUSSION

The shell oscillations calculated in this paper proved to be a fine tool for analyzing the quasi-particle distribution near the Fermi level. Of particular interest is the dependence of the residual interaction on the quasi particle's orbital angular momentum:

$$\delta\varepsilon \sim \hat{\vec{\ell}}^{2} \cong \left(\ell + \frac{1}{2}\right)^{2}. \qquad (59)$$

Only the ℓ^2 dependence of the width of the diffuse Fermi distribution turned out to be compatible with experimental data. This is as it should be in some respects. Since we are dealing with a scalar effect, it must be expressed in terms of the scalar square of the momentum vector.

According to Eq. (55), relatively small angular momenta have an important role. In this respect Eq. (59) can be considered the first term of the expansion in powers of ℓ/p_f. But why is the zero term of the expansion, which is independent of ℓ, missing in this case? Could this mean that the residual interaction in a nucleus with finite radius depends on the additional, apart from energy, integrals of motion of the quasi particle? Unfortunately, a final answer cannot be given to these questions yet. It would be desirable, nonetheless, to point out the difficulties that would presumably arise in attempting to reconcile the current situation with the Cooper effect[14,23] in nuclear matter. In fact, this effect is characterized by the constant width of the statistical distribution's transition region, which is identical for all quasi particles near the Fermi level. It is easy to show, however, that the presence of this constant component in the

transition region's width would eliminate the experimentally observed magic cusps. Therefore, the available experimental data favor more simple and natural hypotheses of the energy spectrum for infinite nuclear matter. It seems that it is an ordinary Fermi liquid with a sharp Fermi level for quasi particles.[13,14]

The type of residual interaction described by Eq. (59), however, is associated with spherical nuclei with a finite radius. Experimental data create the impression that this type of residual interaction gradually decreases with distance from the magic nucleus and finally somehow rearranges itself. The thermodynamic aspects of the transition were investigated by Nosov.[7] The fact that the nucleus is no longer spherical as a result of residual interaction of the phase transition* should not be surprising. It was shown earlier (see Ref. 19) that in a simple scheme without interaction the region is completely unstable in the case of any number of particles.

---

* The critical decrease of the residual interaction having the structure (59) probably occurs when very few quasi-particle states reach the diffuse Fermi distribution region [for example, interaction zone II in the case of the Racah-Mottelson model (28) and (36); see Fig. 5].

APPENDIX

In the calculations above we used a model with a wall impenetrable to quasi particles, situated at a distance R from the center of the nucleus (see Ref. 19). The roots in Fig. 3 of the wave equation for the free motion of a particle in the spherical region correspond to the same boundary condition. We shall show that this is not connected with any constraints imposed on the generality of the results for the shell oscillations of the energy of a spherical nucleus.

In the Bohr-Sommerfeld quantization rule (12) for determining the eigenvalues, the integrand is given by

$$k_\ell(\tau) = \sqrt{k^2 - \frac{\tilde{\ell}^2}{\tau^2}}. \qquad (A1)$$

Because of the uniformity of nuclear matter the wave number k is constant in the inner region. The additional phase γ depends on the properties of the actual structure of the transition layer at the nuclear surface. We shall use the dimensionless variable $kr = \rho'$:

$$\int_{\tilde{\ell}}^{\rho} \sqrt{1 - \frac{\tilde{\ell}^2}{\rho'^2}}\, d\rho' = \pi\,(n + \gamma). \qquad (A2)$$

The Regge trajectories responsible for the oscillations are characterized by the correlation

$$2n + \ell = p, \qquad p = 2, 3, 4, 5..., \qquad \text{(A3)}$$

between the quantum numbers (see Introduction and Fig. 3). Therefore

$$\frac{dn}{d\tilde{\ell}} = -\frac{1}{2}, \qquad \frac{d^2n}{d\tilde{\ell}^2} = 0. \qquad \text{(A4)}$$

Let us differentiate (A2) along the trajectory:

$$\sqrt{1 - \frac{\tilde{\ell}^2}{\rho^2}} \frac{d\rho}{d\tilde{\ell}} - \arccos\frac{\tilde{\ell}}{\rho} = -\frac{\pi}{2} + \pi\frac{d\gamma}{d\tilde{\ell}}. \qquad \text{(A5)}$$

It follows from this that the derivative $d\rho/d\tilde{\ell}$ vanishes at $\tilde{\ell} = 0$ [the last term on the right-hand side, which is determined by differentiating the phase correction, does not affect the result; see Eq. (A7) below]. In the second differentiation of the Bohr-Sommerfeld equation the vanishing terms are dropped:

$$\sqrt{1 - \frac{\tilde{\ell}^2}{\rho^2}} \frac{d^2\rho}{d\tilde{\ell}^2} + \frac{\frac{1}{\rho}}{\sqrt{1 - \frac{\tilde{\ell}^2}{\rho^2}}} = \pi\frac{d^2\gamma}{d\tilde{\ell}^2}. \qquad \text{(A6)}$$

We now take into account the fact that the γ phase is determined by the specific nuclear interactions in the immediate vicinity of the upper limit of integration. Here, any characteristics influencing the result depend on the momentum $\tilde{\chi}$ only in combination with $\tilde{\chi}^2$. Therefore,

$$\frac{d\gamma}{d\tilde{\ell}} = \frac{d\gamma}{d\tilde{\ell}^2} \cdot 2\tilde{\ell}, \qquad \frac{d^2\gamma}{d\tilde{\ell}^2} = 2\frac{d\gamma}{d\tilde{\ell}^2} \sim \frac{1}{\rho^2}. \qquad \text{(A7)}$$

Hence, at $\tilde{\chi} = 0$ of the maximum we get

$$\frac{d^2\rho}{d\tilde{\ell}^2} \cong -\frac{1}{\rho}, \qquad \text{(A8)}$$

if the terms $\approx 1/\rho^2$ are neglected. Thus, Eq. (3)

$$\Delta\rho \cong -\frac{\left(\ell + \frac{1}{2}\right)^2}{2\rho} \qquad \text{(A9)}$$

is independent of the specific structure of the nuclear surface.

Let us now determine the ordinates of the successive trajectories. At $\tilde{\chi} = \ell + 1/2 = 0$, according to (A3), n = p/2 + 1/4. Substituting it in (A2), we get

$$\rho_{max} = \pi\left(\frac{p}{2} + \gamma'\right), \tag{A10}$$

where $\gamma' = \gamma + 1/4$. Substituting $k_f R = \rho_f$ for ρ_{max} we can see that (A10) coincides with the quantization rule (22) (see footnote on p. 15) for the magic values of this parameter (see Ref. 11).

Table 1

Theoretical and Experimental Nucleon Magic Numbers

p	N	N_{theor}		
		(1)	(2)	(3)
2	2	11	15	12
3	8	18	22	19
4	28	30	33	30
5	50	50	52	50
6	82	82	82	81
7	126	129	126	127
8	184(?)	195	187	191
9		281	270	276
10		392	376	386

Table 2

Characteristics of the Residual
Interaction Between Nucleons
(Quasi Particles) Determined From
the Magic Cusps ($\overline{\delta\epsilon}$ is in MeV)

p	N,Z	Neutron magic numbers				Proton magic numbers			
		$\sqrt{\omega}$	g'	g	$\overline{\delta\epsilon}$	$\sqrt{\omega}$	g'	g	$\overline{\delta\epsilon}$
4	28	2.4	2.7	3.3	5.2	1.8	2.2	2.6	3.8
5	50	1.6	2.0	2.3	3.3	1.5	1.9	2.2	2.6
6	82	1.4	1.8	2.0	2.6	1.0	1.5	1.6	1.6
7	126	1.1	1.6	1.7	1.9				

Table 3

The Values of $\delta\varepsilon$ (in MeV) for Specific ℓ

ℓ \ p	4		5		6		7
	$\delta\varepsilon_{neutron}$	$\delta\varepsilon_{proton}$	$\delta\varepsilon_{neutron}$	$\delta\varepsilon_{proton}$	$\delta\varepsilon_{neutron}$	$\delta\varepsilon_{proton}$	$\delta\varepsilon_{neutron}$
0	0.4	0.3			0.14	0.08	
1			1.9	1.5			0.8
2	10.2	7.5			3.5	2.1	
3			10.2	8.1			4.3

Fig. 1   The smooth part of the mass described by Weizsäcker's
         equation has no characteristic features; it is taken
         as the origin of the shell effect schematically repre-
         sented here.   A more detailed and precise plot would
         contain all the curves corresponding to the different
         chemical elements (see, for example, Ref. 6).   The
         mass curve exhibits analogous and equally pronounced
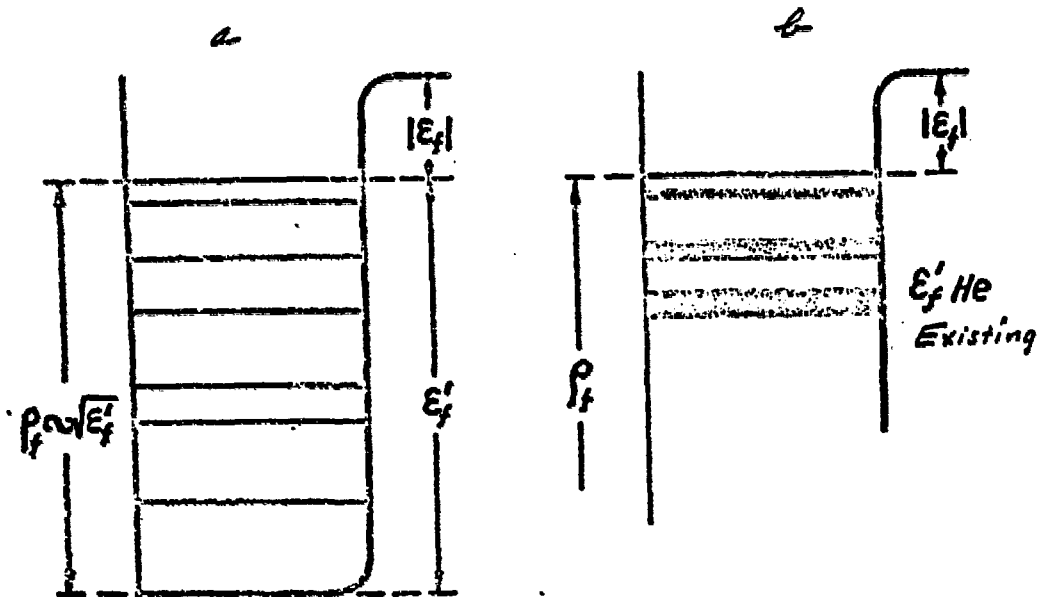   characteristics, depending on the number of protons Z.

Fig. 2 Since the increase (2b) in attenuation (width) of the
single-quasi-particle states in a real Fermi liquid
precludes a correct determination of the location of
the potential well's bottom, case (b), in contrast to
case (a), has only the quasi-particle energy, which is
measured from zero kinetic energy of the free nucleon.
In this highly schematic diagram the quasi-particle
levels are discrete. In fact, the main results in the
following sections [see, for example, Eqs. (19) and
(20)] were obtained in a "macroscopic" approximation
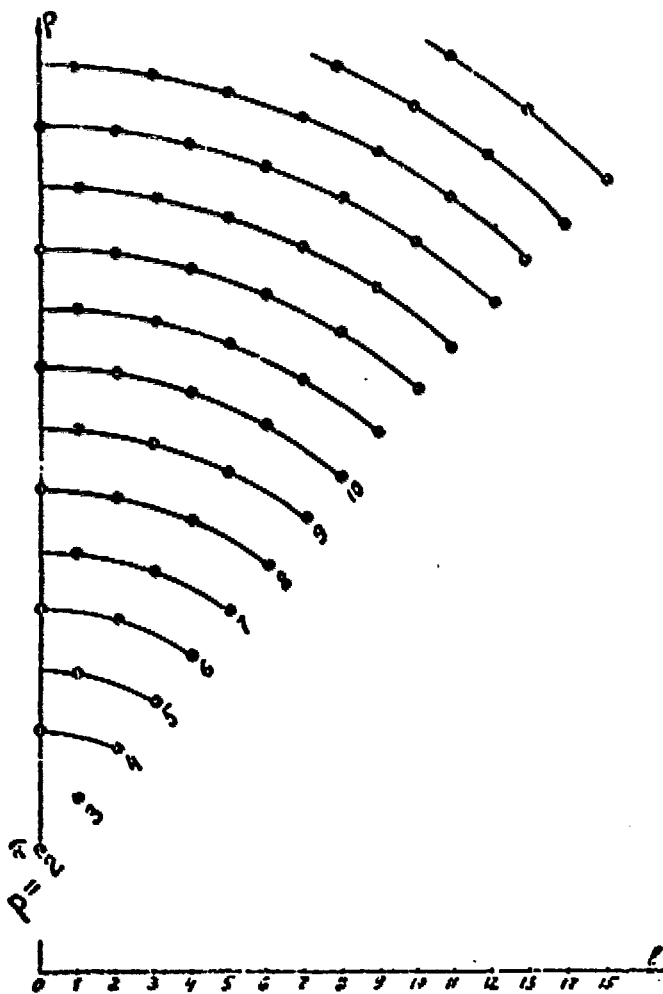in which the energy spectrum of the quasi particles is
continuous.

Fig. 3   The zero-points of the spherical Bessel functions $j_e(\rho)$
are on the l,ρ plane (see Section 2 and Introduction).
The quasi-particle attenuation (see Fig. 2) was not
taken into account. The shell oscillations are deter-
mined by the nearest neighborhood $p \approx p_f$ of the Fermi
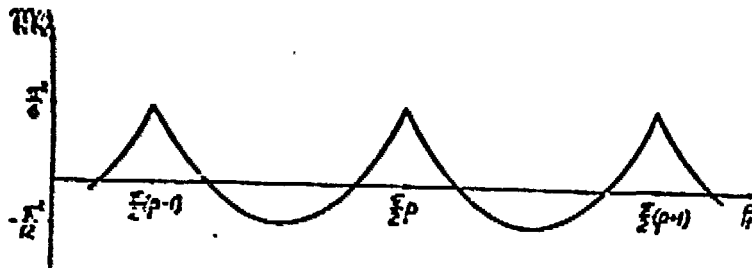level where the corresponding width is negligible.

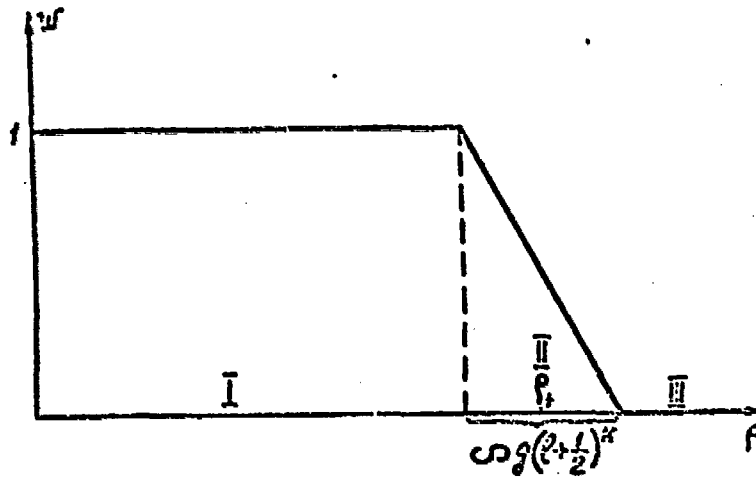Fig. 4 Plot of the $m(\rho_f)$ function [see Eqs. (21) and (23)].

Fig. 5 The Racah-Mottelson model [Hamiltonian (28)] for the
nucleus. The particle-state distribution is given
here for a fixed value of $\widehat{\gamma}$ (or $\widetilde{\beta}$). The $w(\rho,\widehat{\beta})$
distribution function has a characteristic feature
at $\rho = \rho_f$ and $\widetilde{\beta} = 0$ [see Eqs. (36) and (41)], which
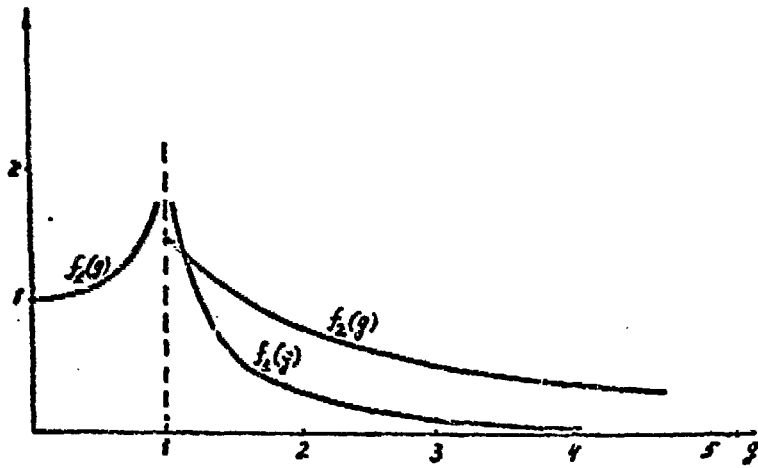is difficult to depict on a plane graph.

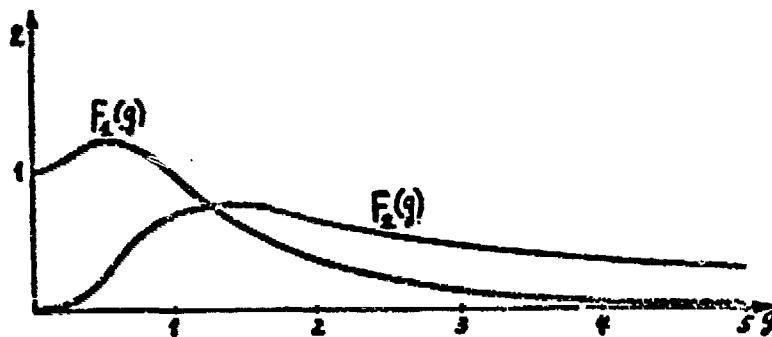Fig. 6 Plots of the $f_1(g)$ and $f_2(g)$ functions [see Eq. (43)].

Fig. 7 Plots of the $F_1(g)$ and $F_2(g)$ functions [see Eq. (49)].

REFERENCES

1. C.F. Weizsäcker, J. Phys., $\underline{96}$, 431 (1935).

2. H. Bethe and P. Becher, Nuclear Physics, publ. by DHTVU, Moscow, 1938.

3. E. Fermi, Nuclear Physics, IL, 1951.

4. M.G. Mayer and J.H. Jensen, Elementary Theory of Nuclear Shell Structure, Wiley, N.Y., 1955.

5. A. Bohr and B. Mottelson, Nuclear Structure, Vol. 1, W.A. Benjamin, N.Y. 1969.

6. W. Myers and W. Swiatecki, Nucl. Phys., $\underline{81}$, 1 (1966).

7. V.G. Nosov, J.E.T.P., $\underline{53}$, 579 (1957).

8. P.E. Hodgeson, Optical Model of Inelastic Scattering, Atomizdat, 1966.

9. A.N. James et al., Nucl. Phys., $\underline{A138}$, 145 (1969).

10. T. Regge, Nuovo Cimento, $\underline{8}$, 671 (1958); $\underline{14}$, 951 (1959).

11. V.G. Nosov and A.M. Kamchatnov, J.E.T.P., $\underline{61}$, 1303 (1971).

12. L.D. Landau and E.M. Lifshitz, Quantum Mechanics, Fizmatgiz, 1963.

13. L.D. Landau, J.E.T.P., $\underline{30}$, 1058 (1956).

14. L.D. Landau and E.M. Lifshitz, Statistical Physics, Fizmatgiz, 1964.

15. R. Courant and D. Hilbert, Methods of Mathematical Physics, Interscience, N.Y., 1953.

16. W.J. de Haas and P.M. van Alphen, Communs. Phys. Lab. Univ. Leiden, $\underline{212a}$, 1930.

17. I.M. Lifshitz and A.M. Kosevich, Dokl. Akad. Nauk, USSR, $\underline{96}$, 963 (1954); J.E.T.P., $\underline{29}$, 730 (1955).

18. J. Rainwater, Phys. Rev., $\underline{79}$, 432 (1951).

19. V.G. Nosov, J.E.T.P., $\underline{57}$, 1765 (1969).

20. G.E. Brown, Unified Theory of Nuclear Models and Forces, Amsterdam, North-Holland Pub. Co., N.Y., 1971.

21. N.K. Bary, A Treatise on Trigonometric Series, Fizmatgiz, 1961.

22. V.A. Kravtsov, Atomic Masses and Nuclear Binding Energy, Atomizdat, 1965.

23. L.N. Cooper, Phys. Rev., $\underline{104}$, 1189 (1956).